Macromolecular Rapid Communications
www.mrc-journal.de

Chiral Binaphthylbis(4,4′-Bipyridin-1-Ium)/Cucurbit[8] Uril Supramolecular System and Its Induced Circularly Polarized Luminescence

Xu-Man Chen, Yong Chen, Lu Liang, Qiu-Jun Liu, and Yu Liu**

Circularly polarized luminescence (CPL) induced by host–guest complexation remains a challenge in supramolecular chemistry. Herein, a couple of CPL–silent enantiomeric guest binaphthylbis(4,4′-bipyridinium) salts can emit obvious CPL in the presence of cucurbit[8]uril in aqueous media, due to the restriction of molecular rotation limitation effect. Such CPL can be reversibly adjusted by the addition of acid and base. Furthermore, the resultant supramolecular systems can interact with DNA, accompanied by the morphological conversion from branched supramolecular nanowires to exfoliated nanowires, which can enable to the exploration of such supramolecular systems as DNA markers by CPL signals.

1. Introduction

Host–guest complexation is an effective way for inducing, enhancing and adjusting various optical properties such as UV–vis absorbance, fluorescence, and circular dichroism (CD).[1] Circularly polarized luminescence (CPL), which is derived from the difference in emission between left and right circularly polarized light by chiral luminophores, has attracted more and more interest.[2] CPL property can bring potential applications in the molecular sensing, asymmetric synthesis, and optical storage devices.[3] Normally, intense CPL signals are achieved from helical organic molecules[4] or chiral lanthanide complexes,[5] and most of these CPL systems are fabricated in the solid state[6] or organic phase.[7] Meanwhile, it is also noted that helical supramolecular complexes constructed from chiral subcomponents can provide a more powerful tool to produce desired optical properties, such as CD and CPL.[8–10]

In the previous studies, numerous rigid supramolecular assemblies have been successfully fabricated by the synergetic combination of cucurbit[8]uril (CB[8]) with 4,4′-bipyridin-1-ium (BP) units.[11] Through the strong complexation of CB[8] with BP units, the fluorescence of guest molecules can be enhanced, mainly due to the restriction of molecular rotation limitation effect. Inspired by these helical supramolecular assemblies, we designed two chiral and cationic (*R*/*S*)-1,1′-binaphthalene derivatives ((*R*)-**1** and (*S*)-**1**) as the guest molecules (**Scheme 1**) to interact with cucurbit[8]uril (CB[8]) as a host molecule in aqueous media. Owing to the chirality of cationic π-expanded binaphthalene derivative tethered by CB[8], the complex of CB[8] with (*R*)-**1** or (*S*)-**1** possess the obvious CPL emission and the amplified anisotropy factor of CD, and the reversible CPL emission of **1**/CB[8] complexes can be adjusted by acid/base. Furthermore, the obtained chiral **1**/CB[8] complexes can further interact with DNA with retentive CPL signals and thus can be used to mark CPL signals on DNA.

2. Experimental Section

2.1. Materials

All the chemical reagents were purchased from commercial resources unless noted. 1 M HCl and 1 M NaOH were used in acid-base responsiveness experiments.

2.2. Synthesis

2.2.1. Synthesis of (R/S)-1

(*R*)-**1** (*(R)-1,1″-([1,1′-binaphthalene]-2,2′-diyl)bis([4,4′-bipyridin]-1-ium)) chloride*): (*R*)-[1,1′-binaphthalene]-2,2′-diamine (0.500 g, 1.30 mmol) and 1-(2,4-dinitrophenyl)- [4,4′-bipyridin]-1-ium chloride (1.500 g, 4.18 mmol) were dissolved in ethanol (40 mL), and the solution was heated to reflux for 72 h. After cooling to room temperature, the solvents was removed via rotary evaporation under reduced pressure, and the resulting residue was purified by column chromatography (CH_2Cl_2:methanol = 1:1) to yield (*R*)-**1** (228 mg, 20.4%), a dark

X.-M. Chen, Dr. Y. Chen, L. Liang, Q.-J. Liu, Prof. Y. Liu
College of Chemistry
State Key Laboratory of Elemento-Organic Chemistry
Nankai University
Tianjin 300071, P. R. China
E-mail: chenyong@nankai.edu.cn; yuliu@nankai.edu.cn
Dr. Y. Chen, Prof. Y. Liu
Collaborative Innovation Center of Chemical Science and Engineering (Tianjin)
Tianjin 300071, P. R. China
The ORCID identification number(s) for the author(s) of this article can be found under https://doi.org/10.1002/marc.201700869.

DOI: 10.1002/marc.201700869

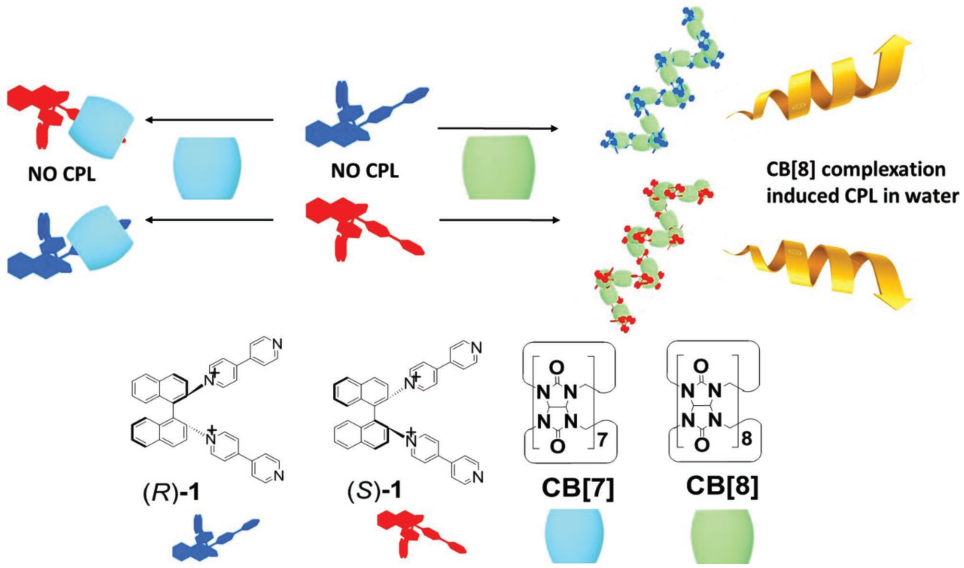

Scheme 1. Schematic illustration of (*R*)-**1**, (*S*)-**1**, CB[8], and the formation of homochiral **1**/CB[8] complexes.

brown powder. HRMS: *m/z* 282.1160, 563.2216 ([(*R*)-**1**]$^{2+}$, calcd for $C_{40}H_{28}N_4^{2+}$, 282.3380, [(*R*)-**1**–H]$^+$, calcd for $C_{40}H_{28}N_4^+$, 563.6680). ^{1}H NMR (400 MHz, D_2O): δ 8.68 (d, 4H), 8.52 (s, 4H), 8.39 (d, 2H), 8.24–8.10 (m, 6H), 7.80 (t, 2H), 7.74 (d, 4H), 7.71–7.60 (m, 4H), 7.52 (m, 2H).

(*S*)-**1** (*(S)-1,1″-([1,1′-binaphthalene]-2,2′-diyl)bis([4,4′-bipyridin]-1-ium)) chloride*): (*S*)-**1** was synthesized with a method similar to that of (*R*)-**1** (yield: 243 mg, 21.7%). HRMS: *m/z* 282.1160, 563.2220 ([(*S*)-**1**]$^{2+}$, calcd for $C_{40}H_{28}N_4^{2+}$, 282.3380, [(*S*)-**1**–H]$^+$, calcd for $C_{40}H_{28}N_4^+$, 563.6680). ^{1}H NMR (400 MHz, D_2O): δ 8.68 (d, 4H), 8.52 (s, 4H), 8.39 (d, 2H), 8.30–8.13 (m, 6H), 7.81 (t, 2H), 7.74 (d, 4H), 7.71–7.61 (m, 4H), 7.52 (m, 2H).

2.3. Methods

2.3.1. NMR Spectroscopy

^{1}H and ^{13}C NMR spectra were recorded on a Brucker AV400 spectrometer.

2.3.2. Fluorescence Spectroscopy

Steady state fluorescence spectra were recorded in a conventional quartz cell (light path 10 mm) on a Varian Cary Eclipse equipped with a Varian Cary single-cell peltier accessory to control temperature.

2.3.3. UV/Vis Spectroscopy

UV/vis spectra and the optical transmittance were recorded in a quartz cell (light path 10 mm) on a Shimadzu UV-3600 spectrophotometer equipped with a PTC-348WI temperature controller.

2.3.4. Transmission Electron Microscopy (TEM) Microscopy

High-resolution TEM images were acquired using a Tecnai 20 high-resolution transmission electron microscope operating at an accelerating voltage of 200 keV. The sample for high-resolution TEM measurements was prepared by dropping the solution onto a copper grid. The grid was then air-dried.

2.3.5. Scanning Electron Microscopy (SEM) Microscopy

SEM images were obtained using a Hitachi S-3500N scanning electron microscope. The sample for SEM measurements was prepared by dropping the solution onto a silicon wafer. The wafer was then air-dried. The SEM samples for control experiment were prepared by direct freezing of the dropped solution on the wafer in liquid nitrogen followed by lyophilization. The resulting cryo-dried materials were imaged after sputtering.

2.3.6. Dynamic Light Scattering (DLS) Spectroscopy

Solution samples were examined on a laser light scattering spectrometer (BI-200SM) equipped with a digital correlator (TurboCorr) at 636 nm at a scattering angle of 90°. The hydrodynamic diameter (Dh) was determined by DLS experiments at 25 °C.

2.3.7. CD Spectroscopy

CD spectra were recorded on a BioLogic MOS500 spectropolarimeter in a quartz cell of 10 mm light path.

2.3.8. CPL Spectroscopy

CPL spectra were recorded in a conventional quartz cell (light path 10 mm) on a JASCO CPL-200 circularly polarized fluorescence spectrometer accessory to control temperature, slit width, and intensity of the light source.

2.3.9. Electrospray Ionization Mass Spectra (ESI-MS) Spectroscopy

ESI-MS were measured by Agilent 6520 Q-TOF-MS.

2.3.10. Preparation of the Sample for Agarose Gel Electrophoresis Analysis

In the experiment, ct-DNA was used in UV/vis spectroscopy experiments, and plasmid DNA pBR322 was used as the model DNA for agarose gel electrophoresis analysis. A mixture of DNA (0.2 μg μL^{-1}) and aqueous samples was incubated at room temperature. All solutions were stored at 4 °C before use.

3. Results and Discussion

We designed a couple of enantiomeric guest compounds (*R*)-**1** and (*S*)-**1** by utilizing the 1:2 binding motif between CB[8] and BP units.[12] First, the inclusion complexation between (*R*)-**1** and (*S*)-**1** with CB[8] was investigated. A theoretical calculation demonstrated that two BP units from different **1** molecules were entrapped in the CB[8] cavity with a head-to-tail orientation[11a] as illustrated in Figures S11 and S12 of the Supporting Information. Job's plots confirmed that two enantiomeric complexes both adopted the 1:1 stoichiometry (Figures S1 and S2, Supporting Information), and the association constants (K_a) could be calculated as 1.62×10^7 M^{-1} for (*R*)-**1**/CB[8] and 6.13×10^7 M^{-1} for (*S*)-**1**/CB[8] using a nonlinear least-squares curve-fitting method by analyzing the sequential changes in the UV–vis absorbance of (*R*)-**1** or (*S*)-**1** in the presence of varying concentrations of CB[8], respectively (**Figure 1**). These obtained K_a values were slightly lower than the corresponding value between phenyl 4,4′-bipyridin-1-ium with CB[8].[11a,12] The decrease of K_a was mainly attributed to the steric hindrance of two BP units. In the ^{1}H NMR spectra, the signals of either free (*R*)-**1** or (*S*)-**1** were broadened with the addition of CB[8] (Figures S3 and S4, Supporting Information). In addition, the interactions of enantiotopic guest molecules with CB[7] as a reference compound were also investigated. ^{1}H NMR experiments showed the obvious peak shifts of (*R*)-**1** or (*S*)-**1** protons with the addition of CB[7] (Figures S5 and S6, Supporting Information). Surprisingly, the association of (*R*)-**1** or (*S*)-**1** with CB[7] also gave a 1:1 binding stoichiometry, and the K_a values were 4.93×10^4 M^{-1} for (*R*)-**1**/CB[7] and 4.01×10^4 M^{-1} for (*S*)-**1**/CB[7] (Figures S7 and S8, Supporting Information). This indicated that only one BP unit in **1** was included, but the other one was located out of the CB[7] cavity (Figures S9 and S10, Supporting Information).

Due to the good optical property of binaphthalene derivatives originated from the expanded π-conjugated system via the rigid modification of BP units and the intermolecular charge transfer (CT), the complexes showed significant chiral optical behaviors. As seen in **Figure 2**, the circular dichroism spectrum of (*S*)-**1** had three peaks at 310, 356, and 400 nm assigned to the signals of binaphthalene units, CT transition and n–π* transition, respectively. With the addition of CB[7], the signal of CT transition disappeared, while the signal of n–π* transition was amplified. This phenomenon may indicate that only one BP unit of (*S*)-**1** was included in by CB[7], which could restrain the CT transition of two BP units in (*S*)-**1** and meanwhile promote the n–π* transition of each BP unit. In the circular dichroism spectrum of (*S*)-**1**/CB[8], the signal of binaphthalene underwent a full inversion. Moreover, the signal of CT transition was greatly enhanced, but the signal of n–π* transition disappeared. These phenomena jointly indicated that two BP units from different (*S*)-**1** molecules were included in the same CB[8] cavity, leading to the stronger CT transition and the weaker n–π* transition. Figure S13 of the Supporting Information shows the detailed changes in the CD spectra of **1** in the presence of CB[8]. A possible explanation for the inverse circular dichroism signals may be the different dihedral angles of **1** with CB[7] and CB[8], which were shown in the optimized structure (Figures S11 and S12, Supporting Information).[13] Moreover, the anisotropy factor of (*S*)-**1**, (*S*)-**1**/CB[8], (*S*)-**1**/CB[7] over the spectral range were calculated on the basis of the equation $g = \Delta A/A = \theta$ [mdeg]/(32980 × A). Figure 2b showed a total inversion between (*S*)-**1**/CB[8] and (*S*)-**1**/CB[7], and the maximum absolute value of anisotropy factor was calculated as 4.83×10^{-3} at 414 nm of (*S*)-**1**/CB[8], which was 5.14 times higher than that of (*S*)-**1**/CB[7]

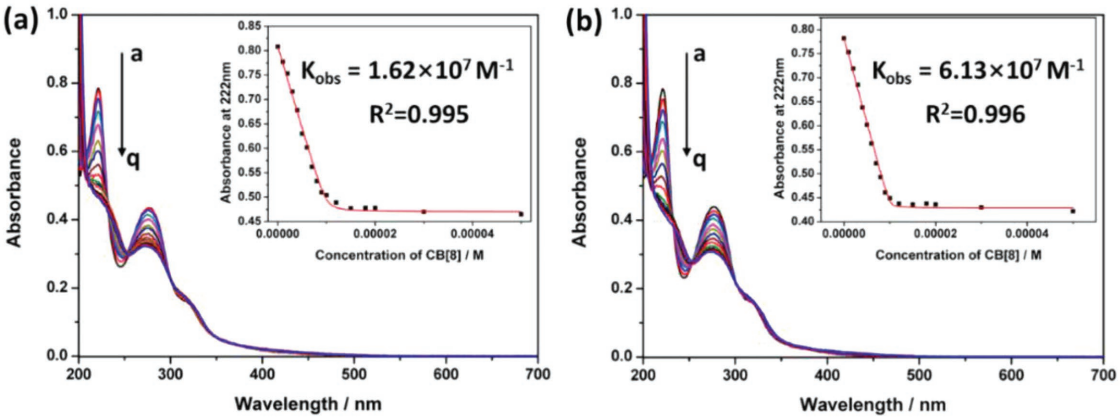

Figure 1. Alternation of UV–vis spectra of a) (*R*)-**1** (10×10^{-6} M), and b) (*S*)-**1** (10×10^{-6} M) upon addition of CB[8] (0×10^{-6}–50×10^{-6} M, from (a) to (q), in aqueous solution at 25 °C. Inset: the nonlinear least-squares analysis of the variation of absorbance with the concentration of CB[8] to calculate the binding constant.

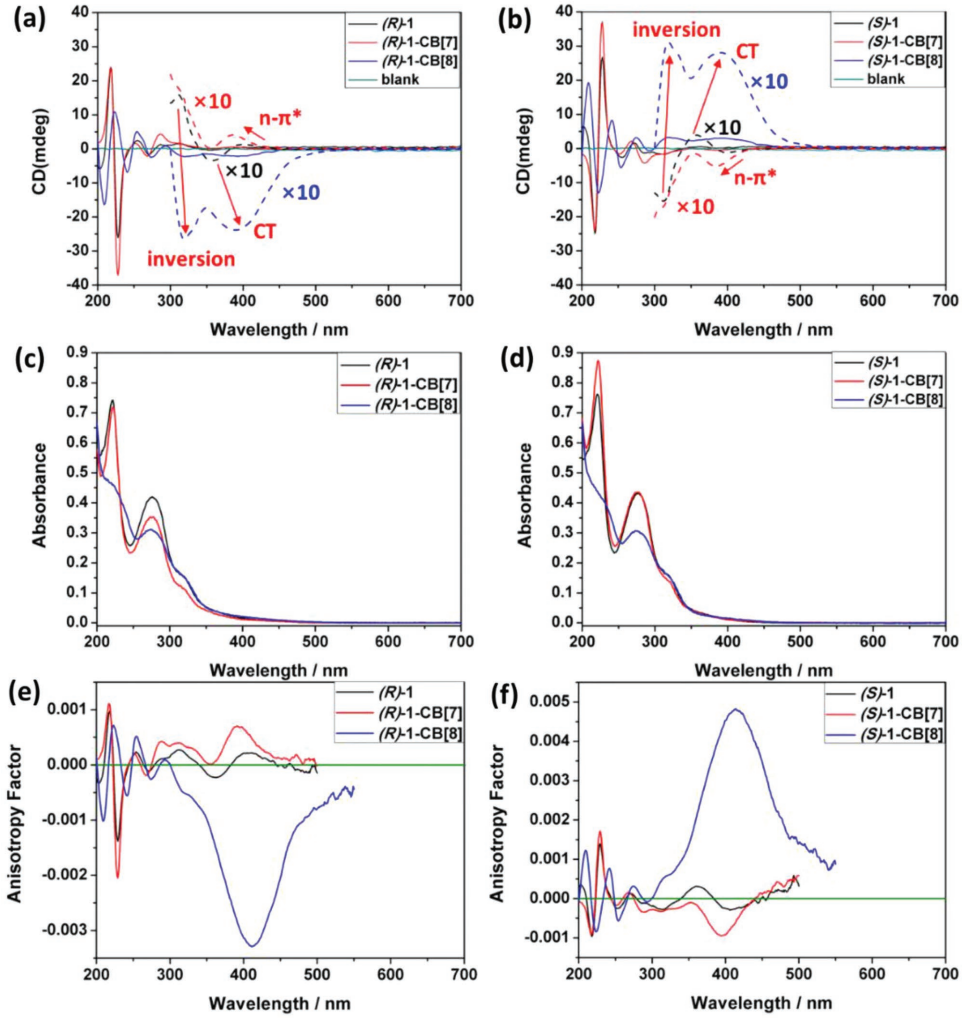

Figure 2. a,b) Circular dichroism spectra, c,d) corresponding UV–vis spectra, and e,f) anisotropy factors of (*R*/*S*)-**1**, (*R*/*S*)-**1** with CB[7], (*R*/*S*)-**1** with CB[8] in aqueous solution ((a,c,e) for (*R*)-**1** and (b,d,f) for (*S*)-**1**). Concentrations of (*R*)-**1**, (*S*)-**1**, CB[7], and CB[8] solutions in (a–d) are 0.01×10^{-3} M. Anisotropy factors in (e) and (f) are calculated from 200 to 450 nm for (*R*/*S*)-**1**, (*R*/*S*)-**1**/CB[7], and from 200 to 500 nm for (*R*/*S*)-**1**/CB[8], respectively. Green lines in (e) and (f) are baselines.

complex (9.4×10^{-4} at 394 nm) and 16.66 times higher than that of (*S*)-**1** (2.9×10^{-4} at 406 nm). Usually, the values of anisotropy factor induced by π–π^* transition are around 10^{-4}, like the anisotropy factor observed in the wavelength region <300 nm (Figure 2f). The unusual anisotropy factor at 414 nm may be resulted from the strong CT transition between two BP units included in the same CB[8] cavity. In this chiral tethered donor–acceptor system, the confined dimer formation may be another factor to enhance the anisotropy factors in charge transfer transition.[14] The corresponding experiments and calculations of (*R*)-**1** were also performed, showing similar circular dichroism inversion between (*R*)-**1**/CB[8] and (*R*)-**1**/CB[7] complexes. In addition, the maximum absolute value of anisotropy factor was up to 3.29×10^{-3} at 413 nm for (*R*)-**1**/CB[8] complex, which was 4.70 times higher than that of (*R*)-**1**/CB[7] complex (0.70×10^{-3} at 391 nm) and 14.95 times higher than that of (*R*)-**1** (0.22×10^{-3} at 405 nm).

Fluorescence variation is considered as one of the basic properties of supramolecular intramolecular charge transfer system. In Figure S14 of the Supporting Information, the emission intensity of **1**/CB[8] enhanced ≈5 times than free **1** and **1**/CB[7], probably due to the encapsulation-enhanced fluorescence enhancement by CB[8] and/or the aggregation induced emission. Significantly, the CPL measurements of (*R*)-**1**/CB[8] complex (**Figure 3**a,b) showed a wide negative peak centered at 550 nm, whereas a mirror CPL signal appeared for (*S*)-**1**/CB[8] complex. The λ_{max} of CPL signal was consistent with that of fluorescence emission spectra, and the $|g_{lum}|$ values for (*R*/*S*)-**1** with CB[8] were 5.07×10^{-3} and 5.38×10^{-3}, respectively. By contrast, no obvious CPL signals could be observed in the case of (*R*/*S*)-**1** or (*R*/*S*)-**1**/CB[7], due to the free rotation of the single bond in **1** and the weaker fluorescence (Figure 3d–f). Therefore, we can deduce that the tethered environment of (*R*/*S*)-**1** by CB[8] complexation is responsible for the CPL emission.

The morphological information of **1**/CB[8] complexes comes from SEM, TEM, and DLS. The diameter of each single nanofiber was about 2.8 nm, which is proved by small-angle

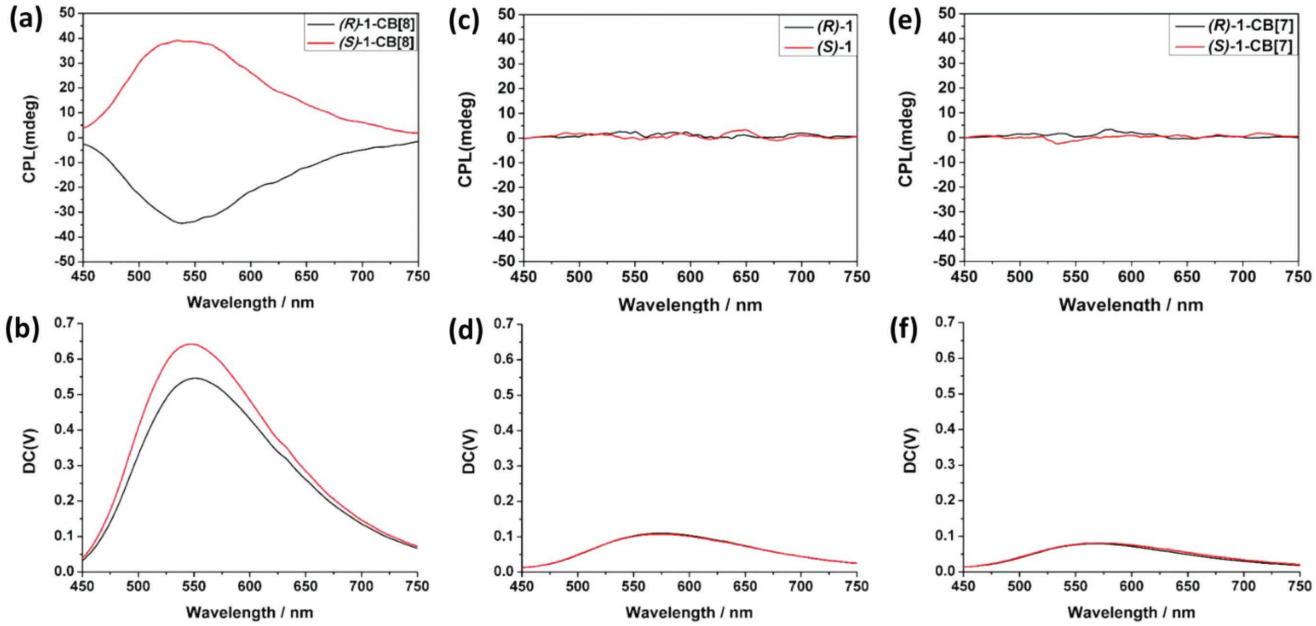

Figure 3. CPL spectra and PL spectra of a,b) (*R*/*S*)-**1** with CB[8], c,d) (*R*/*S*)-**1**, and e,f) (*R*/*S*)-**1** with CB[7] in aqueous solution, respectively. (Concentrations of (*R*)-**1**, (*S*)-**1**, CB[8], CB[7] solutions are all 0.1×10^{-3} M and $\lambda_{ex} = 330$ nm.)

X-ray scattering experiments and optimized geometries (Figures S15 and S12a, Supporting Information). Then, these nanofibers were interconnected with each other through the π–π stacking of numerous binaphthalene units, which are located at the periphery of nanofibers, to form nanobundles with several micrometers in length (Figure S16, Supporting Information). TEM images (Figure S17, Supporting Information) also showed a number of parallel nanofibers and nanobundles. In comparison, either the homochiral **1** or the homochiral **1**/CB[7] could be assembled to nanoparticles with an average diameter of 200–300 nm (Figure S18, Supporting Information), which was basically consistent with DLS data, i.e., 199 nm for (*R*)-**1**, 200 nm for (*S*)-**1**, 312 nm for (*R*)-**1**/CB[7] and 290 nm for (*S*)-**1**/CB[7] (Figure S19, Supporting Information). The average hydrodynamic diameters of (*R*)-**1**/CB[8] (806 nm) or (*S*)-**1**/CB[8] (990 nm) were much larger than those of (*R*)-**1**, (*S*)-**1**, (*R*)-**1**/CB[7], and (*S*)-**1**/CB.[7].

Some further experiments were carried out to investigate the smart control of CPL. Because of the reversible protonation and deprotonation behaviors of nitrogen atoms on BP units in **1**/CB[8] complexes,[12] CPL signals could be efficiently and reversibly quenched and recovered. In a typical example, 10 equivalents of HCl were added to (*R*/*S*)-**1**/CB[8] system. As a result, the fluorescence and CPL intensities obviously decreased, and UV–vis spectra and circular dichroism spectra changed slightly (**Figure 4**; Figures S20 and S21, Supporting Information). When increasing the amount of HCl to 100 equivalents, both fluorescence and CPL signals quenched, and a new peak appeared at 450 nm in the circular dichroism spectra assigned to the protonated BP units. With the further addition of NaOH, UV–vis, circular dichroism, fluorescence, and CPL signals recovered to the original levels. SEM images also displayed the acid/base-responsive disaggregation and regeneration of complexes (Figure S22, Supporting Information).

Possessing positive charges, **1**/CB[8] complexes could interact with DNA, which was confirmed by the agarose gel electrophoresis assay with pBR 322 DNA. In a typical example, **1**/CB[8] gave a good interaction ability with DNA other than free **1** (**Figure 5**a,b). It is noteworthy that the CPL signals of homochiral **1**/CB[8] underwent no obvious changes after interacting with DNA, indicating that the host–guest complexation of CB[8] and **1** was stable in the DNA binding process (Figure 5c,d). Thus, such chiral complexes could mark DNA by CPL signals. Meanwhile, UV–vis and CD intensities were almost unchanged after the addition of DNA in **1**/CB[8] (Figures S23 and S24, Supporting Information) When pBR 322 DNA was added, the DNA chains could wind around the nanofiber of **1**/CB[8] owing to the electrostatic interaction between the negatively charged DNA and the positively charged **1**/CB[8] This phenomenon subsequently avoided the π–π stacking and the hydrophobic interactions among the nanofibers, and thus led to the exfoliated nanofibers as observed in SEM images (Figure S25, Supporting Information).

4. Conclusions

In summary, we report a CB[8]-induced circularly polarized luminescence of binaphthalene derivatives in aqueous media due to the restriction of molecular rotation limitation. The CPL signals of such complexes can be reversibly controlled by acid and base. In addition, these complexes can interact with DNA and act as a CPL marker of DNA. The present work provides a pathway for the design of supramolecular CPL complexes as bioprobes in water.

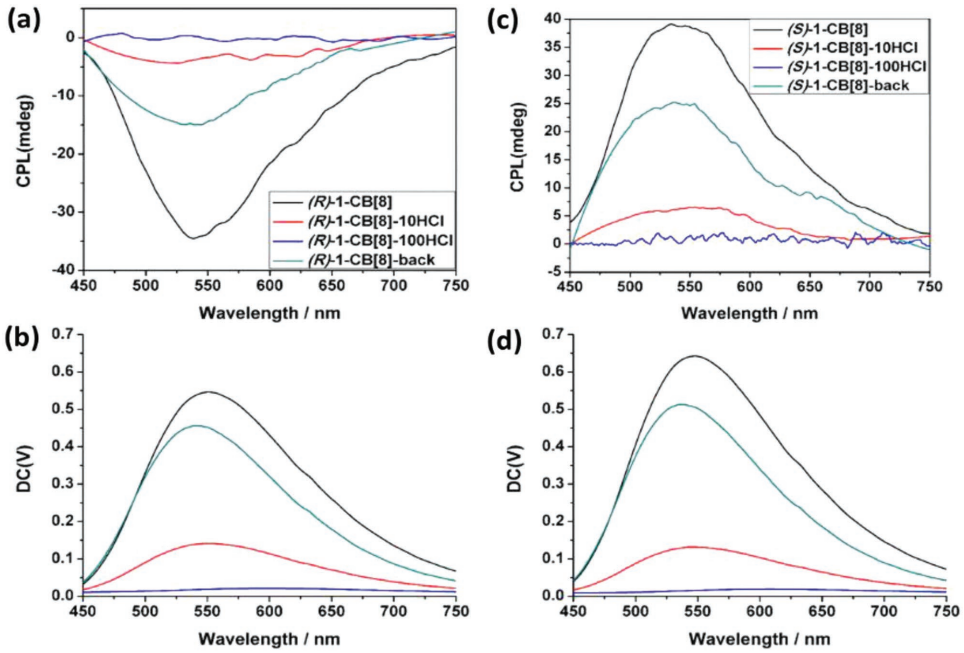

Figure 4. a,b) CPL and PL spectra of (*R*)-**1** (0.1×10^{-3} M) with CB[8] (0.1×10^{-3} M), adding 10 and 100 equiv. of HCl to this complex solution and adjusting pH back to original state. c,d) CPL and PL spectra of (*S*)-**1** (0.1×10^{-3} M) with CB[8] (0.1×10^{-3} M) corresponding with (*R*)-**1** with CB[8].

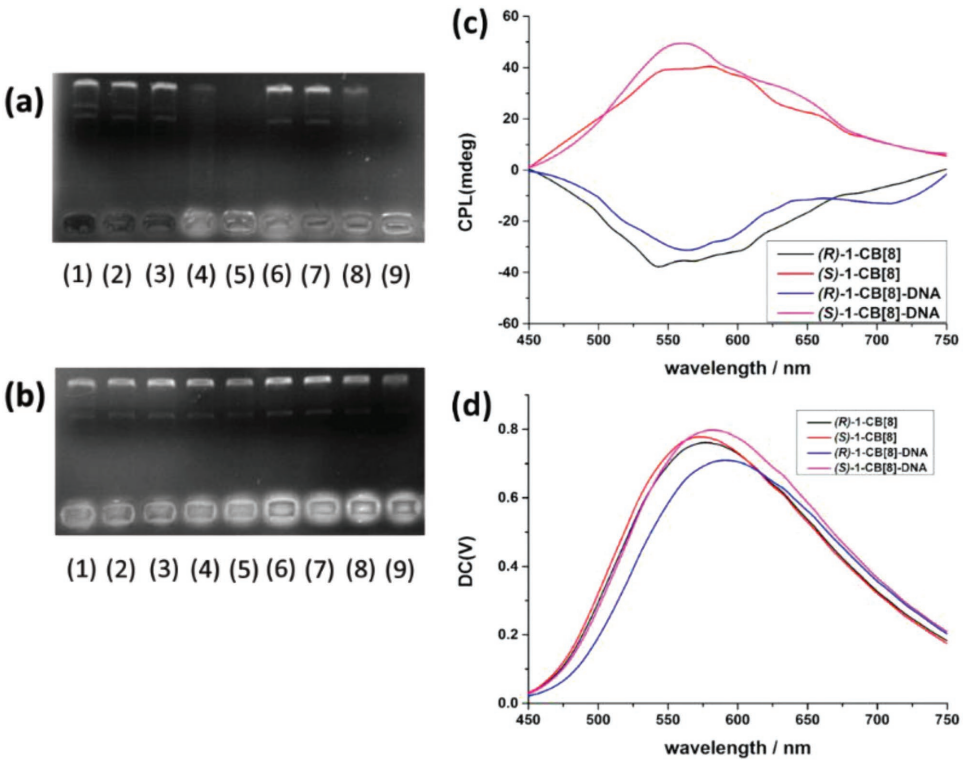

Figure 5. Agarose gel electrophoresis assay to investigate the interaction of DNA with a) (*R*/*S*)-**1** and CB[8] (1:1) b) (*R*/*S*)-1:lane (1), DNA alone; lanes (2–5) (*R*)-**1** and CB[8] or without CB[8]; lanes (6–9) (*S*)-**1** and CB[8] or without CB[8]. The DNA concentration is 12 ng/μL. The different concentrations of (*R*/*S*)-**1** and CB[8] (1:1) from lane 2 to lane 5 are 5, 10, 50, 100×10^{-6} M, and different concentrations of (*R*/*S*)-**1** from lane 6 to lane 9 are 5, 10, 50, 100×10^{-6} M, respectively. c) CPL and d) PL spectra of *(R)*-**1** or *(S)*-**1** (0.1×10^{-3} M) with CB[8] (0.1×10^{-3} M) and pBR 322 DNA (12 ng μL^{-1}) in aqueous solution, respectively. ($\lambda_{ex} = 330$ nm.)

Supporting Information

Supporting Information is available from the Wiley Online Library or from the author.

Acknowledgements

The authors thank NNSFC(21432004, 21672113, 21772099, and 91527301) for financial support.

Conflict of Interest

The authors declare no conflict of interest.

Keywords

circularly polarized luminescence, cucurbit[8]uril, DNA markers, supramolecular chemistry

Received: December 20, 2017
Revised: February 9, 2018
Published online: March 12, 2018

[1] a) L. You, D. J. Zha, E.V. Anslyn, *Chem. Rev.* **2015**, *115*, 7840; b) C. Liu, D. Yang, Q. Jin, L. Zhang, M. Liu, *Adv. Mater.* **2016**, *28*, 1644; c) Y. Zhou, H. Y. Zhang, Z. Y. Zhang, Y. Liu, *J. Am. Chem. Soc.* **2017**, *139*, 7168; d) H. Wu, Y. Chen, Y. Liu, *Adv. Mater.* **2017**, *29*, 1605271; e) Q. W. Zhang, D. F. Li, X. Li, P. B. White, J. Mecinović, X. Ma, H. Ågren, R. J. M. Nolte, H. Tian, *J. Am. Chem. Soc.* **2016**, *138*, 13541; f) M. Inouye, K. Hashimoto, K. Isagawa, *J. Am. Chem. Soc.* **1994**, *116*, 5517; g) A. C. Bhasikuttan, J. Mohanty, W. M. Nau, H. Pal, *Angew. Chem., Int. Ed.* **2007**, *46*, 4120.

[2] a) G. Snatzke, *Angew. Chem., Int. Ed.* **1979**, *18*, 363; b) N. Berova, L. D. Bari, G. Pescitelli, *Chem. Soc. Rev.* **2007**, *36*, 914; c) F. S. Richardson, J. P. Riehl, *Chem. Rev.* **1977**, *77*, 773; d) M. Schadt, *Annu. Rev. Mater. Sci.* **1997**, *27*, 305; e) J. G. Bünzli, C. Piguet, *Chem. Soc. Rev.* **2005**, *34*, 1048.

[3] a) R. Carr, N. H. Evans, D. Parker, *Chem. Soc. Rev.* **2012**, *41*, 7673; b) J. Roose, B.-Z. Tang, K. S. Wong, *Small* **2016**, *12*, 6495; c) F. Zinna, M. Pasini, F. Galeotti, C. Botta, L. Di Bari, U. Giovanella, *Adv. Funct. Mater.* **2017**, *27*, 1603719; d) N. Hellou, M. Srebro-Hooper, L. Favereau, F. Zinna, E. Caytan, L. Toupet, V. Dorcet, M. Jean, N. Vanthuyne, J. A. G. Williams, L. Di Bari, J. Autschbach, J. Crassous, *Angew. Chem., Int. Ed.* **2017**, *56*, 8236.

[4] a) E. M. Sánchez-Carnerero, A. R. Agarrabeitia, F. Moreno, B. L. Maroto, G. Muller, M. J. Ortiz, S. de la Moya, *Chem. Eur. J.* **2015**, *21*, 13488; b) R. Aoki, R. Toyoda, J. F. Kögel, R. Sakamoto, J. Kumar, Y. Kitagawa, K. Harano, T. Kawai, H. Nishihara, *J. Am. Chem. Soc.* **2017**, *139*, 16024.

[5] R. Carr, N. H. Evansa, D. Parker, *Chem. Soc. Rev.* **2012**, *41*, 7673.

[6] a) J. Zhang, W. C. Feng, H. X Zhang, Z.-L. Wang, H. A. Calcaterra, B. Yeom, P. A. Hu, N. A. Kotov, *Nat. Commun.* **2016**, *7*, 10701; b) M. Shimada, Y. Yamanoi, T. Ohto, S. T. Pham, R. Yamada, H. Tada, K. Omoto, S. Tashiro, M. Shionoya, M. Hattori, K. Jimura, S. Hayashi, H. Koike, M. Iwamura, K. Nozaki, H. Nishihara, *J. Am. Chem. Soc.* **2017**, *139*, 11214; c) K. Takaishi, T. Yamamoto, S. Hinoide, T. Ema, *Chem. Eur. J.* **2017**, *23*, 9249.

[7] a) J. R. Brandt, X. H. Wang, Y. Yang, A. J. Campbell, M. J. Fuchter, *J. Am. Chem. Soc.* **2016**, *138*, 9743; b) E. M. Sánchez-Carnerero, F. Moreno, B. L. Maroto, A. R. Agarrabeitia, M. J. Ortiz, B. G. Vo, G. Muller, S. de la Moya, *J. Am. Chem. Soc.* **2014**, *136*, 3346.

[8] a) E. Yashima, N. Ousaka, D. Taura, K. Shimomura, T. Ikai, K. Maeda, *Chem. Rev.* **2016**, *116*, 13752; b) L. C. Palmer, S. I. Stupp, *Acc. Chem. Res.* **2008**, *41*, 1674.

[9] a) A. Samanta, Z. Liu, S. K. M. Nalluri, Y. Zhang, G. C. Schatz, J. F Stoddart, *J. Am. Chem. Soc.* **2016**, *138*, 14469; b) T. Kaseyama, S. Furumi, X. Zhang, K. Tanaka, M. Takeuchi, *Angew. Chem., Int. Ed.* **2011**, *50*, 3684.

[10] a) J. Kumar, T. Nakashima, T. Kawai, *J. Phys. Chem. Lett.* **2015**, *6*, 3445; b) M. Inouye, K. Hayashi, Y. Yonenaga, T. Itou, K. Fujimoto, T. Uchida, M. Iwamura, K. Nozaki, *Angew. Chem., Int. Ed.* **2014**, *53*, 14392; c) D. Yang, P. F. Duan, L. Zhang, M. H. Liu, *Nat. Commun.* **2017**, *8*, 15727.

[11] a) K. Zhang, J. Tian, D. Hanifi, Y. Zhang, A. C. H. Sue, T. Y. Zhou, L. Zhang, X. Zhao, Y. Liu, Z.-T. Li, *J. Am. Chem. Soc.* **2013**, *135*, 17913; b) S. Q. Xu, X. Zhang, C. B. Nie, Z. F. Pang, X. N. Xu, X. Zhao, *Chem. Commun.* **2015**, *51*, 16417; c) X. M. Chen, Y. M. Zhang, Y. Liu, *Supramol. Chem.* **2016**, *28*, 817.

[12] Z. J. Zhang, H. Y. Zhang, Y. Liu, *J. Org. Chem.* **2011**, *76*, 4682.

[13] Y. Sheng, D. Shen, W. Zhang, H. Zhang, C. Zhu, Y. Cheng, *Chem. Eur. J.* **2015**, *21*, 13196.

[14] T. Mori, Y. Inoue, *Angew. Chem., Int. Ed.* **2005**, *44*, 2582.